Tang *et al. Satellite Navigation* (2022) 3:26
https://doi.org/10.1186/s43020-022-00087-x

Satellite Navigation
https://satellite-navigation.springeropen.com/

ORIGINAL ARTICLE Open Access

Analysis of GPS P(Y) signal power enhancement based on the observations with a semi-codeless receiver

Xiaomei Tang*, Muzi Yuan and Feixue Wang

Abstract

The Global Position System (GPS) satellites of Block IIR-M and later versions can turn on the signal power enhancement if needed. In recent years, this power enhancement has been triggered several times when the U.S force was involved in local conflicts, which was observed by the monitoring receivers at International GNSS Service (IGS)/international GNSS Monitoring and Assessment System (iGMAS) stations or the high-gain antennas at monitoring ground stations. The specific power enhancement magnitudes with these two observation methods are different. The observations of L1/L2 P(Y) power with a high-gain antenna are accurate, while the observations at IGS/iGMAS stations contain biases. This paper analyses the reasons for the observation biases with monitoring receivers at IGS/iGMAS stations and proposes a method verifying the accurate relation between the observed carrier-to-noise ratio (C/N_0) data and the real power enhancement magnitudes. When the power enhancement event happens, the observed L1/L2 P(Y) C/N_0 data at IGS/iGMAS stations can be corrected using the model proposed in this paper. In the analysis, this paper concludes that the power of L1P(Y) increases by about 4.3–5.3 dB and the power of L2P(Y) by about 4.6–5.2 dB in power enhancement events, which matches the designed capability of GPS satellites as well. The results are also verified by the data of high-gain antennas.

Introduction

In order to improve the anti-jamming capability of the navigation service in conflict environments, the power enhancements of GPS L1 P(Y) signal and L2 P(Y) signal were used many times. The power enhancement of GPS signals and its influence on GNSS services were reported and studied (Fan et al., 2012; Jiménez-Baños et al., 2011). The latest enhancement event in Syria was also analysed in many works (Thoelert et al., 2018; Xie et al., 2021). In these studies, the data from International GNSS Service (IGS) stations are used. However, at these stations, as long as most non-military users, the real power increment of each signal component cannot be obtained by its observed C/N_0, because the P(Y) signals are received with semi-codeless methods.

The semi-codeless and codeless methods of receiving GPS L1P(Y) and L2P(Y) signals are widely discussed (Betz & Cerruti, 2020; Liao et al., 2006; O'Driscoll & Curran, 2017; Soloviev et al., 2012; Zeng et al., 2017). Montenbruck et al. (2006) compared the performance of three different dual-frequency receivers equipped with semi-codeless receiving algorithms. The research indicates that the complexity and the accuracy of tracking are various in these three receivers. Woo (2000) also compared the performance of several codeless and semi-codeless tracking receivers. The result shows that the z-track has the least C/N_0 loss among them. Borio (2011) analysed the performance of squaring and cross-correlation in the tracking of GPS L2P(Y) signal and proposed a generalized codeless PLL structure. Borio et al. (2013) and Borio (2019) also developed the method of codeless processing

*Correspondence: txm_nnc@126.com

College of Electronic Science, National University of Defense Technology, Changsha, Hunan Province, China

Springer Open

© The Author(s) 2022. **Open Access** This article is licensed under a Creative Commons Attribution 4.0 International License, which permits use, sharing, adaptation, distribution and reproduction in any medium or format, as long as you give appropriate credit to the original author(s) and the source, provide a link to the Creative Commons licence, and indicate if changes were made. The images or other third party material in this article are included in the article's Creative Commons licence, unless indicated otherwise in a credit line to the material. If material is not included in the article's Creative Commons licence and your intended use is not permitted by statutory regulation or exceeds the permitted use, you will need to obtain permission directly from the copyright holder. To view a copy of this licence, visit http://creativecommons.org/licenses/by/4.0/.

of the BOC (Binary Offset Carrier) signal, and other researchers analysed the performance of most codeless and semi-codeless tracking algorithms (Bakholdin et al., 2020; Betz & Cerruti, 2020). Besides, the voting modulation method used in GPS III satellites may influence the performance of codeless tracking method and was analysed in Allen et al. (2020). Based on these analyses, most tracking stations nowadays adapt the z-track method for L1P(Y) and L2P(Y) signal tracking because of its better C/N_0 performance.

The signal power enhancement events are also studied by several works. Jiménez-Baños et al. (2011) analysed the change in signal power level during September 7 to September 12, 2010. Thoelert et al. (2018) analysed the signal power distribution of L1P(Y) between February 7 and 8 2017 using the data of GNSS receivers combined with high-gain antennas. The result shows that during the enhancement period the signal power of different components is redistributed for all GPS IIR-M satellites so that the power of L1P signal increases while the L1M decreases. Sun et al. (2011) analysed the influence of signal power increment in positioning performance and gave the upper bound for power increment. In addition, some researchers have also analysed the authorized signals of GNSS systems using the data from high-gain antennas (He et al., 2020; Lestarquit et al., 2012; Xiao et al., 2018; Yan et al., 2019). However, in these papers, the model calculating power increment of L1P(Y) and L2P(Y) is based on the approximate evaluation of frequency spectrum magnitudes, but this evolution is not authentically precise.

Nowadays, researchers adopt the increase in C/N_0 estimation as the actual power enhancement of GPS signals. But this may introduce a bias related to the structure of the z-track algorithm, which is widely adopted for the receivers at IGS stations in receiving P(Y) signals. For example, Table 2 demonstrates the C/N_0 increments observed at different stations. Take ARUC station as an example, the C/N_0 observation of GPS L2P(Y) of PRN1 increased by 9.1070 dB during the operation. However, the research (Li et al., 2011) tells that GPS Block II-F satellites do not have the capability to achieve a power enhancement greater than 7 dB. Hence, if the change in C/N_0 observation is adopted as the power enhancement, there will be a bias in the estimation. Besides, these IGS stations are not equipped with high-gain antennas especially parabolic antennas. There are no reliable Power Spectrum Density (PSD) observations at these stations to make any analysis. Thus, an unbiased method to estimate the power enhancement of P(Y) signal is needed.

The better understanding of GPS power enhancement strategy may guide developers to make better receivers and provide the suggestions for other GNSS to improve their power enhancement capability. To reduce the bias of power enhancement estimation using the z-track method and to provide an accurate estimation when a high-gain antenna is not available, this paper refines the power increment result by analysing the model of semi-codeless receiving, and then proposes the equations showing the accurate relation between the observed C/N_0 data and the real power enhancement magnitudes. The signal data from tracking stations and high-gain antennas are used to verify the proposed model.

The rest of this paper is arranged as follows. First, the z-track model is analysed and the method to evaluate the power modification from the z-track results is proposed in "Model and signal power evaluation method of the z-track" section. Then in "Observation data from tracking stations" section, the observation data of various ground stations are analysed, which is the primary conclusion obtained through the theoretical result of the in "Model and signal power evaluation method of the z-track" section. In "Signal data from a high gain antenna" section, the data of high-gain antennas are used to verify the result. In "Discussion and application potential" section, the application and other features in the proposed analyse method is discussed. Finally, the conclusion is drawn in "Conclusion" section.

Model and signal power evaluation method of the z-track

GPS satellites broadcast signals of three frequencies, namely L1, L2, and L5. Although several new signal branches have been developed these years, the L1C/A, L1P and L2C L2P are kept in use on all the working satellites. Among them, L1P and L2P are both modulated by P code only with the difference that P code on L2P is a delayed version of L1P. The P code on GPS L2P(Y) is publicly available, but an additional code is modulo-2 added to P code for the purpose of Anti-Spoofing (AS). This code is known as W code, while the combination of P code and W code is called P(Y) code. The generation of W code is not published but its chip rate is known as 0.5115 MHz.

Since P code and W code are the same in L1 and L2 signals, it is possible to generate P code and track L2P(Y) signal via L1 signal. Based on this assumption, there are many methods to receive GPS L1P(Y) and L2P(Y) signals for non-authentic users, including codeless methods and semi-codeless methods (Wang et al., 2012). In 1992, Ashtech researched how to track L1P(Y) and L2P(Y) signals after Y code is added to the original P code (Ashjaee & Lorenz, 1992). Woo (2000) developed the receiving structure of the z-track for L1P(Y) and L2P(Y) which outperforms the other methods because of its less C/N_0 loss, and the structure of the z-track is shown as Fig. 1. Ashtech used this tracking technique in its receivers.

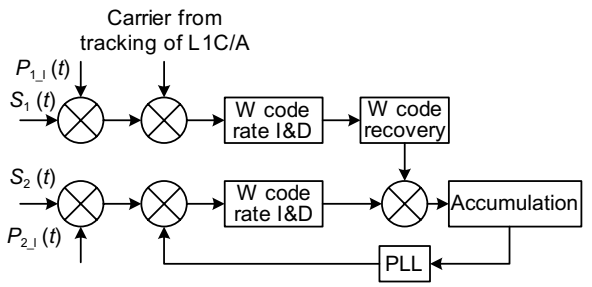

Fig. 1 Digital signal processing structure of the z-track method. Spreading code of L2P(Y) is estimated and accumulated through stable tracking of L1C/A signal

Nowadays, many IGS stations are equipped with Ashtech receivers using the z-track technique (IGS Station Information).

From the upper part of Fig. 1, the z-track utilizes the signal energy of both L1P(Y) and L2P(Y). Since the P(Y) code on L1P signal is partially known, it leads to C/N_0 loss when recovering the carrier. Hence L1C/A is tracked to recover the carrier. After that, L1P is correlated with local P code and integrated into baseband. It should be noticed that L1P is integrated at the rate of W code, which means that the coherent integration length is equal to the time length of W code. Hence W code is recovered from the integration result based on hard decision.

After these procedures, the recovered W code from L1P(Y) is used for tracking L2P(Y) as shown in the bottom part of Fig. 1. L2P(Y) signal is first correlated with P code and integrated at the rate of W code. The integration result of L2P is expressed in Eq. (1), in which the carrier tracking error on L2P is temporarily neglected for convenience:

$$\begin{aligned} I_{\mathrm{nt2\_}i} &= \frac{1}{T_{\mathrm{M}}} \int_{t=(i-1)T_{\mathrm{M}}}^{iT_{\mathrm{M}}} S_2(t) P_{2\_\mathrm{I}}(t)\mathrm{d}t \\ &= \frac{1}{T_{\mathrm{M}}} \int_{t=(i-1)T_{\mathrm{M}}}^{iT_{\mathrm{M}}} (P_2(t)\mathrm{W}_2(i) + n) P_{2\_\mathrm{I}}(t)\mathrm{d}t \\ &= W_2(i) + N_i \end{aligned} \tag{1}$$

where T_M is the chip length of W code, $S_2(t)$ is the signal of L2P(Y), $P_{2\_I}(t)$ is the locally generated P code of L2P, n is white noise, $W_2(i)$ is the *ith* chip of W code with the amplitude of $+1$ or -1, and N_i is the noise after integration.

It should be noted that the correlation loss caused by carrier frequency error and code phase error is ignored since it is not significant when the track loop converges.

Then the integration result is correlated with the W code recovered from L1P(Y) and accumulated. However, the recovered W code from L1P may contain bit errors because of a low C/N_0 of satellite signal. Therefore, the result of accumulation is expressed as Eq. (2) when considering error bits:

$$\begin{aligned} A_{\mathrm{cc2}} &= \frac{1}{K}\sum_{i=0}^{K-1} I_{\mathrm{nt2\_}i} W_1(i) \\ &= \frac{1}{K}\sum_{i=0}^{K-1} (W_2(i) + N_i) W_1(i) \\ &= \frac{1}{K}\sum_{i=0}^{K-1} W_2(i) W_1(i) + \sum_{i=0}^{K-1} N_i M_1(i) \\ &= \frac{1}{K}(K_{\mathrm{Ws}} - K_{\mathrm{Wd}}) + \sum_{i=0}^{K-1} N_i M_1(i) \end{aligned} \tag{2}$$

Here K is the number of accumulated integration results, K_{Ws} is the number of correctly recovered W code chips and K_{Wd} is the number of wrongly recovered W code chips.

Statistically, the number of error chips of W code is determined by the C/N_0 of L1 signal. And this number can be calculated through the Bit Error Rate (BER) of BPSK modulation. These flipped W codes will reduce the correlation result in L2 signal, which finally cause the loss in C/N_0 of L2. If L_C chips are involved in the correlation, the base correlation result should equal to L_C in case no error chip. When the number of error chips is less than $L_C/2$, every single error chip would reduce the correlation result by 2 ($+1$ shift to -1). This loss of correlation result can be calculated as $\mathrm{E}[R_{\mathrm{CNloss}}] = 20\log_{10}(1 - 2R_{\mathrm{BE}})$. The BER can be calculated through BPSK modulation as $R_{\mathrm{BE}} = Q(\sqrt{2R_{\mathrm{CN1}}T_{\mathrm{M}}})$. According to the above analysis the expected accumulation loss can be expressed as follows:

$$\mathrm{E}[R_{\mathrm{CNloss}}] = 20\log_{10}\left(1 - 2Q\left(\sqrt{2R_{\mathrm{CN1}}T_{\mathrm{M}}}\right)\right) \tag{3}$$

where R_{CNloss} is the C/N_0 loss caused by the error bits, and the R_{CN1} is the C/N_0 of L1P. $Q(x)$ is expressed as follows:

$$Q(x) = \int_x^{+\infty} \frac{1}{\sqrt{2\pi}} \exp\left(-\frac{1}{2}t^2\right)\mathrm{d}t \tag{4}$$

Therefore, one can see that the observed C/N_0 of L2P is affected by the C/N_0 of both L1P(Y) and L2P(Y).

The GPS satellites have the capability to increase the transmitting power of signals. The designed transmitting power of different GPS signals in different satellites can be found in Li et al. (2011). It is known from Li's research that the GPS IIR satellites do not have the capability of increasing signal power while GPS IIRM/

IIF in both L1P and L2P do have. In the next part of the evaluation, the C/N_0 increment of L1P and L2P are analysed according to the observation of L2P signal. From the calculation power enhancing capability of GPS IIF L1 and L2 are 6.9 dB and 5.3 dB, respectively.

Based on the analysis in "Model and signal power evaluation method of the z-track" section, if the correlation loss caused by code phase error and carrier frequency error is ignored, the observed C/N_0 of L2P can be expressed as:

$$R_{\mathrm{CN2Obs}} = R_{\mathrm{CN2}} - R_{\mathrm{CNloss}} \tag{5}$$

Hence the change of the estimated C/N_0 of L2P signal is determined by the changes of R_{CN2} and R_{CNloss}, which is expressed as Eq. (6).

$$\begin{aligned} G_{2\mathrm{Obs}} &= (R_{\mathrm{CN2}} - R_{\mathrm{CNloss}})_2 - (R_{\mathrm{CN2}} - R_{\mathrm{CNloss}})_1 \\ &= (R_{\mathrm{CN2}})_2 - (R_{\mathrm{CN2}})_1 - \left((R_{\mathrm{CNloss}})_2 - (R_{\mathrm{CNloss}})_1\right) \end{aligned} \tag{6}$$

Here the subscripts 1 and 2 stand for the observations before and after the power increment, respectively. Figure 2 shows the relation between R_{CNloss} and the C/N_0 of L1P.

It is known from Fig. 2 that the change of R_{CNloss} is approximately linear with the change of L1P C/N_0, which is between 25 and 55 dB·Hz. The relation is expressed as follows:

$$R_{\mathrm{CN2loss}} = 2.62 + (55 - R_{\mathrm{CN1}}) \times 0.944 \tag{7}$$

Substituting Eq. (7) into Eq. (6), the G_{L2PObs} can be expressed as Eq. (8).

$$\begin{aligned} G_{2\mathrm{Obs}} &= (R_{\mathrm{CN2}})_2 - (R_{\mathrm{CN2}})_1 \\ &\quad + ((R_{\mathrm{CN1}})_2 - (R_{\mathrm{CN1}})_1) \times 0.944 \\ &= G_2 + 0.944 \times G_1 \end{aligned} \tag{8}$$

Here $G_{2\mathrm{Obs}}$ is the observed C/N_0 increment of L2P, G_2 is the real C/N_0 increment of L2P, and G_1 is the actual C/N_0 increment of L1P. When the receiving condition does not drastically change, the C/N_0 increment reflects the enhancement of transmitting signal power on the satellite.

Supposing that the signal C/N_0 increments of L1P and L2P are the same (observed in PSD data from high-gain antenna), the G_2 would be identical to the G_1. Therefore, the power increment of L1P and L2P can be expressed as:

$$G_{(L1P,L2P)} = G_{2\mathrm{Obs}}/(1 + 0.944) \tag{9}$$

Here $G_{(L1P,L2P)}$ is the power increment of L1P and L2P. Analyses of the power enhancement of GPS L1P(Y) and L2P(Y) signals will rely on this theoretical result in the rest of the paper.

Observation data from tracking stations

To verify the theoretical deduction, the observation data at different tracking stations are analysed. During the period from April 13 to April 17 in 2018, a signal power increment of L1P(Y) and L2P(Y) was observed at many stations. Hence the signal C/N_0 observations from International GNSS Service (IGS) tracking stations are analysed. During the period of time, an attack mission was operated by American Army and the time relationship between the power enhancement and attack mission is shown in Fig. 3.

As shown in Fig. 3, a preparation stage was from 06:01 to 18:36, afterwards the power enhancement was deployed and then the attack mission started. The chosen IGS tracking stations are shown in Table 1.

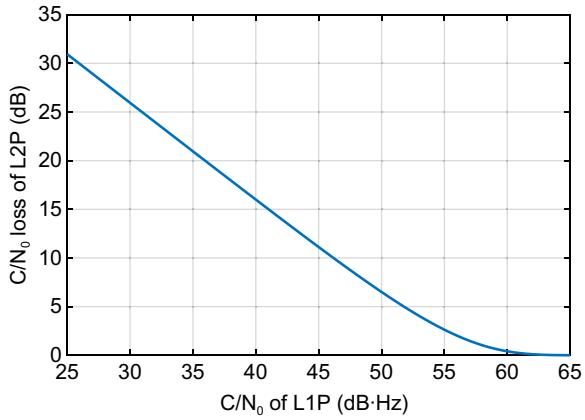

Fig. 2 The relation of loss in tracking C/N_0 vs the C/N_0 of L1P. Loss of tracking C/N_0 drops with the increasement of L1P C/N_0 because there will be fewer bit error when L1P C/N_0 increases

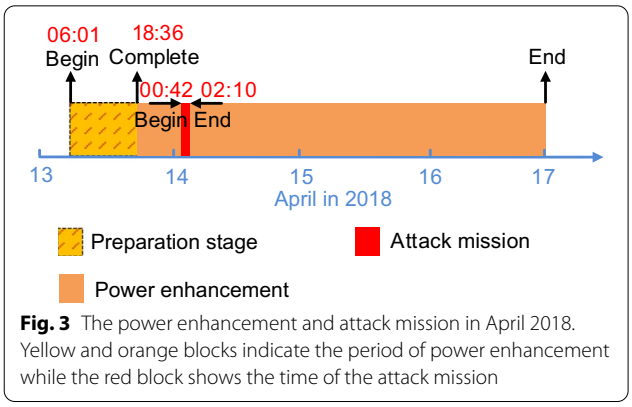

Fig. 3 The power enhancement and attack mission in April 2018. Yellow and orange blocks indicate the period of power enhancement while the red block shows the time of the attack mission

Table 1 Position of chosen IGS stations

Station	Position		
	Longitude (°)	Latitude (°)	Altitude (m)
ARUC	40.29	44.09	1222
DYNG	38.08	23.93	510
CUT0	− 32.00	115.89	24
HARB	− 25.89	27.707	1558
JFNG	30.516	114.49	71.3
KIRU	67.857	20.968	391
UCAL	51.080	− 114.1	1119

The observation data of PRN 2, PRN1, and PRN7 are analysed, in which PRN2 satellite is GPS IIR while PRN 1 is GPS II-F satellite and PRN 7 is GPS IIR-M satellite.

The L2P(Y) signal C/N_0 of GPS PRN2 satellite observed at ANKR for 7 days is shown in Fig. 4, in which time is expressed in weeks while the decimal part is the time in week. The time can be converted to Gregorian calendar date by considering the start point of GPS time, which is 0 h UTC (midnight) of January 6th 1980. For example, day 6 of week 1996 corresponds to April 13, 2018. The figure shows that the C/N_0 of PRN2 remains almost the same, but the L2P(Y) signal C/N_0 of PRN7 increases from April 13, 2018 to April 17, 2018.

Since the repeating period of GPS satellites is 23 h 56 min, the C/N_0 data is shifted by −4 min every day to make time epoch aligned in Fig. 5. The L2P(Y) C/N_0 increment is obtained by calculating the difference between the observed C/N_0 in April 13 and that in April 12. To make the data more reliable, the observed C/N_0 is chosen based on the following principle:

1. The observed C/N_0 data should be taken between a constant tracking stage.

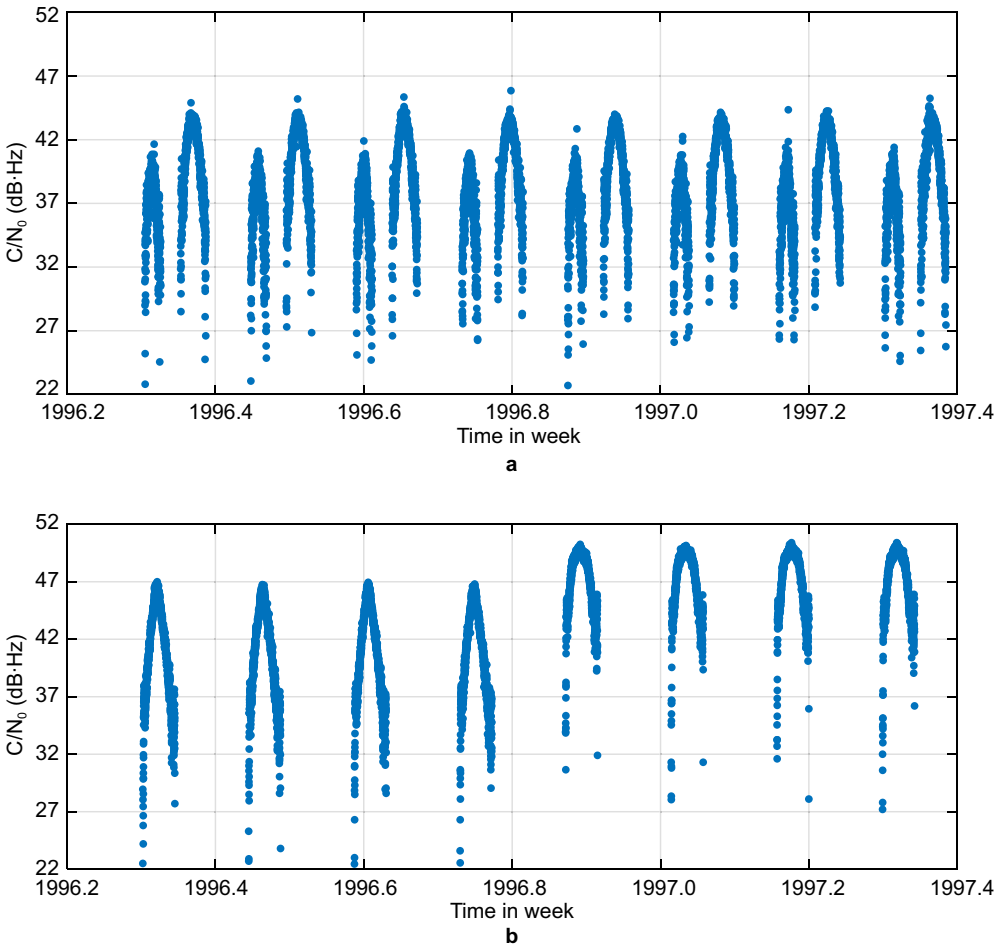

Fig. 4 The L2P(Y) signal C/N_0 observed at ANKR station in seven days; **a** PRN 2 satellite **b** PRN 7 satellite

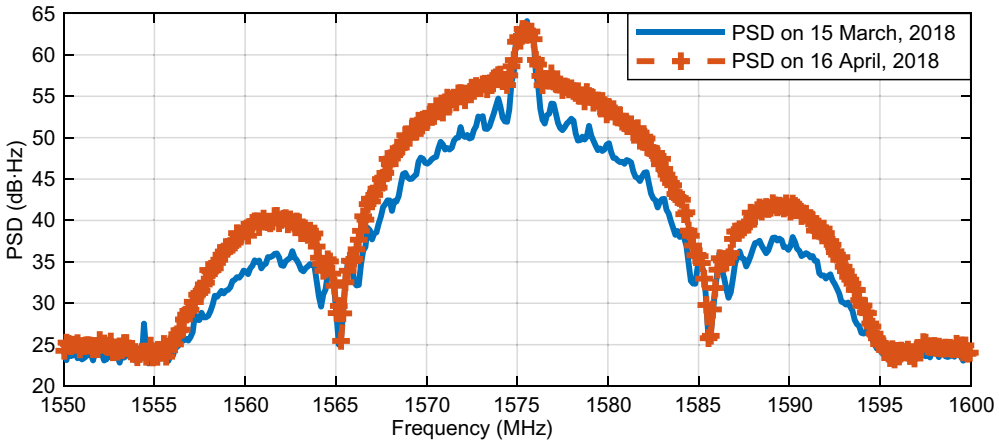

Fig. 5 The PSD of GPS Block IIF-10 L1 signal. The PSD is observed from the samples of a high-gain antenna

2. During the tracking stage, the satellite elevation should be above 15°.

When the these principles are satisfied, $G_{(L1P,L2P)}$ can also be calculated according to the Eq. (9). The C/N_0 increment values are obtained based on the data from different tracking stations considering both PRN 1 and PRN7, which is shown in Table 2. Some conclusions can be drawn from Table 2:

1. The observed C/N_0 increments at different stations vary from 8.5 to 10.4 dB for PRN1. The difference may be caused by the elevation angle of satellite or the C/N_0 estimation methods at different tracking stations. Hence the power increments of L2P are between 4.4 and 5.3 dB considering that the increment of L1P and L2P is identical.
2. The observed C/N_0 increment values at different stations vary from 9.0 to 10.15 dB for PRN 7, while the power increments of L2P are between 4.6 and 5.2 dB.

The analysis result basically matches the designed capability of satellites collected by Li et al. (2011). Besides we found Block IIR-M satellites had similar behaves as Block II-F satellites.

Signal data from a high-gain antenna

The signal data from a high-gain antenna with 40 m calibre at National Time Service Centre of Chinese Academy of Sciences is used to verify the analysis result. The power gain of a parabolic antenna can be calculated with

$$G = \eta\left(\frac{\pi D}{\lambda}\right)^2 \tag{10}$$

Here η is the effectiveness of the antenna, D is the calibre, and λ is the wavelength of the working frequency. For $\eta = 0.65$ and calibre $D = 40$, the antenna has a 26.32 dB gain for GPS L1 in the direction of main lobe. The R_{CN} of GPS L1C/A signal is shown as

Table 2 C/N_0 increment observed from different stations

Station	RINEX edition	PRN1		PRN7	
		G_{2Obs}(dB)	$G_{(L1P,L2P)}$(dB)	G_{2Obs}(dB)	$G_{(L1P,L2P)}$(dB)
ARUC	RINEX 3.0	9.1070	4.6847	10.1576	5.2251
DYNG	RINEX 3.0	8.5913	4.4194	9.8385	5.0610
CUT0	RINEX 3.0	10.4033	5.3515	9.9619	5.1244
HARB	RINEX 3.0	9.3024	4.7852	9.5778	4.9269
JFNG	RINEX 3.0	10.3431	5.3205	9.9940	5.1409
KIRU	RINEX 3.0	8.9880	4.6235	10.0265	5.1577
UCAL	RINEX 3.0	9.3167	4.7925	9.0040	4.6317

$$R_{\mathrm{CN}} = \frac{P_{\mathrm{s}} G_{\mathrm{a}}}{kT} = 73.3\ \mathrm{dB\,Hz} \tag{11}$$

In tracking L1C/A signal, the C/N_0 is estimated and shown in Fig. 6.

From the Fig. 6 we confirm that the quality of the samples from the high-gain antenna meets the theoretical results. Figure 5 shows the PSD of L1 obtained from the high-gain antenna before and after the signal power is increased. From Fig. 5, the signal power of L1C/A is almost the same in these two days with the signal power of L1P(Y) increased by about 5 dB (Steigenberger et al., 2019).

To get the actual increment of signal power, the PSD is integrated while the signal power of L1C/A is excluded. Hence the PSD is integrated between ($f_1-20.46$ MHz, $f_1-1.023$ MHz) and ($f_1+1.023$ MHz, $f_1+20.46$ MHz) where f_1 is the carrier frequency of L1 signal. As is known, L1P(Y) is a BPSK modulated signal that the shape of PSD can be described as sinc(.) function. According to the consistence of the sinc(.) function in the whole frequency interval, one can use the PSD between ($f_1-20.46$ MHz, $f_1-1.023$ MHz) and ($f_1+1.023$ MHz, $f_1+20.46$ MHz) to represent the PSD of the whole L1P(Y) signal. In other word, the spectrum between interval ($f_1-1.023$ MHz, $f_1+1.023$ MHz) will increase or decrease in the same scale as in the interval between ($f_1-20.46$ MHz, $f_1-1.023$ MHz) and ($f_1+1.023$ MHz, $f_1+20.46$ MHz).

The signal power increment can be expressed as

$$G_1 = \int\limits_{f\in f_{\mathrm{span}}} (P_{\mathrm{SD}})_{\mathrm{day2}}\,\mathrm{d}f \Big/ \int\limits_{f\in f_{\mathrm{span}}} (P_{\mathrm{SD}})_{\mathrm{day1}}\,\mathrm{d}f \tag{12}$$

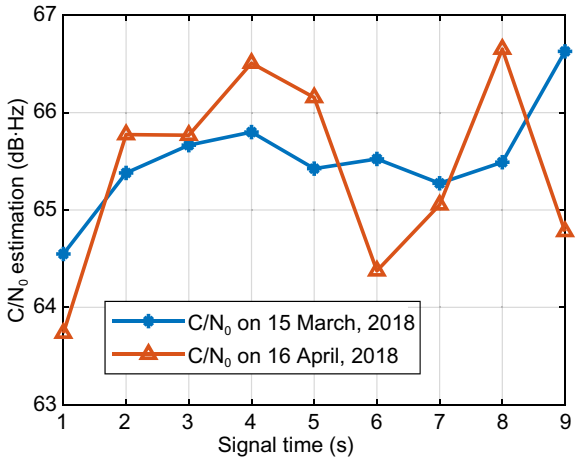

Fig. 6 The C/N_0 estimation of L1C/A signal of GPS Block IIF-10 in high-gain antenna samples. The samples were recorded on 15 March, 2018 and 16 April, 2018

where f_{span} is the PSD integration frequency range shown above, while $(P_{\mathrm{SD}})_{\mathrm{day1}}$ and $(P_{\mathrm{SD}})_{\mathrm{day2}}$ are the PSDs of two days of signals. It can be calculated that G_1 is about 4.47 dB.

Figure 7 shows the PSD of L5 and L2 obtained from the high-gain antenna. It is known from the figure that the PSD of L5 is almost the same in these two days. But for L2, whose signal modulation changes from L2C+L2P+L2M to L2C+L2P, the power of L2C remains the same in two days while the power of L2P significantly increases.

The same method in Eq. (12) is used to calculate the power increment of L2P. In order to avoid the influences of L2M and L2C, the PSD integration frequency span is ($f_2-5.115$ MHz, $f_2-1.023$ MHz) and ($f_2+1.023$ MHz, $f_2+5.115$ MHz), and the calculated G_{L2P} is about 4.078 dB.

By using the values of G_1 and G_2, $G_{2\mathrm{Obs}}$ can be calculated as 8.30 dB. This result matches the results in Table 2 considering the statistical errors in calculating the power increment by the data of the high-gain antenna.

In the above analyses we find there is a about 5 dB of enhancement in P(Y) signals while the power of C/A signals are not influenced. Besides, the signals carrying M code disappeared in the whole process of enhancement. From these results we can speculate that the satellite of GPS IIR-M and later version has an ability to adjust its modulation and power distribution among all components of its transmission. In the Syrian example, we observed the phenomenon that the power of M code signal may be transferred to P(Y) signal. The long-term observation of GPS III satellites may also discover that the power of P(Y) signal can also be transferred to M code signals if needed.

Discussion and application potential

The PSD from a high-gain antenna, especially parabolic antennas is usually used to estimate the signal power of military GNSS signals (Thoelert et al., 2018). However, very few GNSS stations all over the world are equipped with high-gain antennas especially parabolic antennas. For example, IGS stations monitor the GNSS signals via an omnidirectional antenna (e.g., Leica AR10 antenna in ANKR station provides a maximum of 10 dB gain at zenith direction) through C/N_0 observations in tracking channels.

If we want to estimate the power enhancement of P(Y) signals at these stations, the typical method is to observe the change in C/N_0 estimation in tracking channels using the z-track method. However, this estimation method will lead to a bias in the result when power of P(Y) signal increases in both L1 frequency and L2 frequency as

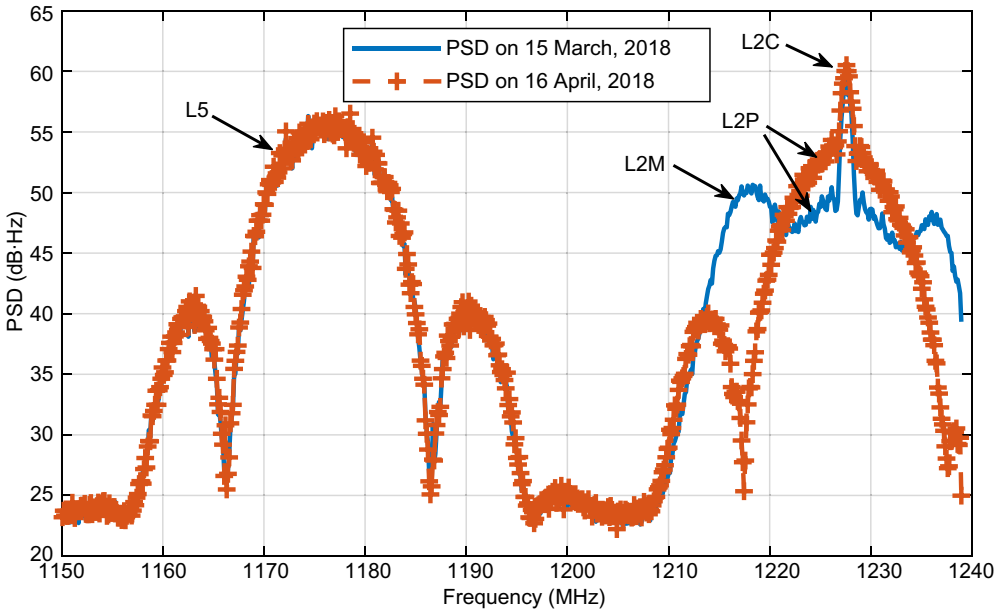

Fig. 7 The PSD of GPS Block IIF-10 L5 and L2 signal. The PSD is observed from samples of high-gain antenna

we have analysed in "Model and signal power evaluation method of the z-track" section. Our work provides an unbiased estimation of the actual power increase scale via C/N_0 estimations in the z-track. This method can provide the capability of estimating the power enhancement for those stations without high-gain antennas. This can give the potential for a global observation network to monitor any power enhancement events in real-time and in every beam of any satellite.

In future, modernized satellites will have more flexible power enhancement capability. Since the power enhancement can occur in just a narrow beam of the satellite, it is possible that no high-gain antenna happens in the beam and is able to receive the enhanced signal. This scenario makes the analysis of signal power possible with no reliable data from high-gain antenna. However, the dense stations of IGS or other observation networks are quite possible to be covered in the enhanced beam and a real-time C/N_0 estimation can be obtained. With the proposed method in this work, an unbiased result such as that derived from high-gain antennas can be drawn just from these C/N_0 observations. This can have a great application potential. Another application of the proposed method is to correct the C/N_0 estimation of P(Y) signal in the existing stations. Influenced by the estimation error of W code, there is a bias in C/N_0 estimation at the existing stations. Initially calibrated via the data from high-gain antennas, these stations will have the capability to continually obtain the unbiased estimation of C/N_0 of P(Y) signal using the proposed method.

Conclusion

Based on the analysis of the z-track method of L1P and L2P, the accurate relation between the observed C/N_0 and the actual power increment magnitude is shown in the paper.

It is known from the signal data of L1P(Y) and L2P(Y) at IGS stations that the power of Block IIR satellites did not change while the signal power of Block IIF satellites increases. By using the proposed relation equation, one can calculate that the power of L1P(Y) increases by about 4.3–5.3 dB and the power of L2P(Y) by about 4.6–5.2 dB. The reason for this result is that the power enhancement in L1P did not reach its capacity (6.9 dB) at that time, mainly intends to make an evenly increase in both L1P and L2P. The signal data of a high-gain antenna is also used to analyse the signal power increment, which shows that the signal power increment of L1P(Y) is about 4.47 dB while that of L2P(Y) is about 4.078 dB.

It can be concluded that the analysis result based on the accurate model proposed in this paper matches the results of the high-gain antenna considering the statistical errors as for the power increment capability of satellites, which matches the designed capability of GPS satellites as well. We also find the flexibility of GPS satellites in power distribution. Hence, the results verify the correctness of the

proposed method to analyse the real C/N_0 increment by using C/N_0 observations based on the z-track method.

Acknowledgements
The authors acknowledged the International GNSS Service (IGS) centre for providing data.

Author contributions
XT provided the initial idea for this work and wrote this manuscript. XT and MY contributed to the analyses of results. XT, MY and FW contributed to the discussions. All authors read and approved the final manuscript.

Funding
The work is supported by the program of National Natural Science Foundation of China (Grant Nos: U20A0193, 62003354).

Availability of data and materials
Seven BDS sites were used in this study: ARUC, DYNG, CUT0, HARB, JFNG, KIRU and ULAB, which are IGS stations. These data are publicly available via the internet (ftp://cddis.gsfc.nasa.gov/).

Declarations

Competing interests
The authors declare that they have no conflict of interest.

Received: 26 December 2021 Accepted: 31 October 2022
Published online: 15 November 2022

References

Allen, D. W., Arredondo, A., Barnes, D. R., Betz, J. W., Cerruti, A. P., Davidson, B., Kovach, K. L., & Utter, A. (2020). Effect of GPS III weighted voting on P(Y) receiver processing performance. *NAVIGATION: Journal of the Institute of Navigation, 67*(4), 675–689. https://doi.org/10.1002/navi.394

Ashjaee, J., & Lorenz, R. (1992). Precise GPS surveying after Y-code. In *Proceedings of the 5th international technical meeting of the satellite Division of the Institute of Navigation (ION GPS 1992)*. Albuquerque, NM, USA (pp. 657–659).

Bakholdin, V. S., Gavrilov, D. A., Dobrikov, V. A., & Ivanov, V. F. (2020). Codeless acquisition of GNSS signals. *Gyroscopy Navigation, 11*(1), 68–76. https://doi.org/10.1134/S2075108720010058

Betz, J. W., & Cerruti, A. P. (2020). Performance of dual-channel codeless and semicodeless processing. *NAVIGATION: Journal of the Institute of Navigation, 67*(1), 109–128. https://doi.org/10.1002/navi.347

Borio, D. (2011). Squaring and cross-correlation codeless tracking: Analysis and generalisation. *IET Radar, Sonar and Navigation, 5*(9), 1–12.

Borio, D. (2019). Cross-correlation codeless processing of BOC modulated signals. *IET Radar Sonar and Navigation, 13*(11), 1998–2007.

Borio, D., Rao, M., & Odriscoll, C. (2013). Codeless processing of binary offset carrier modulated signals. *IET Radar Sonar and Navigation, 7*(2), 143–152.

Fan, J., Li, C., Yuan, L., & Niu, F. (2012). Study on power-enhanced technology of global navigation satellites. In J. Sun, J. Liu, Y. Yang, & S. Fan (Eds.), *China satellite navigation conference (CSNC) 2012 proceedings*. Lecture notes in electrical engineering (Vol. 161). Berlin, Heidelberg: Springer. https://doi.org/10.1007/978-3-642-29193-7_7

He, C., Lu, X., Guo, J., Su, C., & Wang, M. (2020). Initial analysis for characterizing and mitigating the pseudorange biases of beidou navigation satellite system. *Satellite Navigation, 1*(1), 3.

Jimenez-Banos, D., Perelló-Gisbert, J. V., & Crisci, M. (2011) The measured effects of GPS flex power capability collected on sensor station data. In *2010 5th ESA workshop on satellite navigation technologies and European workshop on GNSS signals and signal processing (NAVITEC)*. Noordwijk, Netherlands (pp. 1–6).

Lestarquit, L., Gregoire, Y., & Thevenon, P. (2012). Characterizing the GNSS correlation function using a high gain antenna and long coherent integration—Application to signal quality monitoring. In *Proceedings of the IEEE/ION PLANS 2012*. Myrtle Beach, SC, USA (pp. 877–885).

Li, Z., Zheng, J., & Zhang, L. (2011). *Enlightenment from evolution of the GPS payload for BeiDou system*. CSNC. (in Chinese).

Liao, B., Yuan, H., & Lin, B. (2006). Smoother and bayesian filter based semi-codeless tracking of dual-frequency gps signals. *Science in China Series f: Information Sciences, 49*(4), 533–544.

Montenbruck, O., Garcia-Fernandez, M., & Williams, J. (2006). Performance comparison of semicodeless GPS receivers for LEO satellites. *GPS Solutions, 10*(4), 249–261.

O'Driscoll, C., & Curran, J. T. (2017). Codeless processing of BOC(10,5) signals. In *Proceedings of the 30th international technical meeting of the satellite division of the institute of navigation (ion GNSS+ 2017)*. Portland, Oregon, USA (pp. 3508–3518).

Soloviev, A., Gunawardena, S., & Graas, F. V. (2012). Mitigation of GPS cross-correlation errors using semi-codeless tracking. *IEEE Transactions on Aerospace and Electronic Systems, 48*(1), 502–513.

Steigenberger, P., Tholert, S., & Montenbruck, O. (2019). Flex power on GPS block IIR-M and IIF. *GPS Solutions, 23*(8), 1–12.

Sun, J., Chu, H., & Dong, H. (2011). Research on power-enhanced technology and coverage areas of global navigation satellites. *Acta Geodaetica Et Cartog Raphica Sinica, 40*, 80–84. (in Chinese).

Thoelert, S., Hauschild, A., Steigenberger, P., Langley, R. B., & Antreich, F. (2018). GPS IIR-M L1 transmit power redistribution: Analysis of GNSS receiver and high-gain antenna data. *NAVIGATION: Journal of the Institute of Navigation, 65*(3), 423–430.

Unknown. IGS Station Information—ARTU00RUS. Available at: https://igs.org/imaps/station.php?id=ARTU00RUS.

Wang, X., Sun, Y., Du, Q., Wu, D., & Wang, D. W. (2012). Dynamic-aided L2P(Y) tracking in dual-frequency GPS receiver. *Acta Electronica Sinica, 40*(10), 1938–1942.

Woo, K. T. (2000). Optimum semi-codeless carrier phase tracking of L2. *NAVIGATION: Journal of the Institute of Navigation, 47*(2), 82–99.

Xiao, W., Liu, W. X., Mou, W. H., Yong, L., & Sun, G. F. (2018). Research into a recovery method of GNSS authorized service signal component. *IEEE ACCESS, 6*, 27651–27658.

Xie, C., Xian, D., Li, T., Wang, G., & Wang, Q. (2021). Analysis of GPS signal power enhancement effect based on data from multiple ground stations. In C. Yang, & J. Xie, (Eds.) *China satellite navigation conference (CSNC 2021) proceedings*. Lecture notes in electrical engineering, vol 773. Singapore: Springer. https://doi.org/10.1007/978-981-16-3142-9_1.

Yan, T., Wang, Y., Wang, G., Qu, B., Lei, W., & Meng, Y. (2019). Separation and evaluation method of GNSS authorized service signals. In J. Sun, C. Yang, & Y. Yang (Eds.), *China satellite navigation conference (CSNC) 2019 proceedings. CSNC 2019*. Lecture notes in electrical engineering (Vol. 563). Singapore: Springer. https://doi.org/10.1007/978-981-13-7759-4_30.

Zeng, C., Li, W. M., Bi, B., & Chen, Q. L. (2017). Application of extended Kalman filter based semi-codeless for tracking high dynamic GPS L2 signal. In *2016 IEEE international conference on signal and image processing (ICSIP)*. Beijing, China (pp. 503–507).

Publisher's Note

Springer Nature remains neutral with regard to jurisdictional claims in published maps and institutional affiliations.

Submit your manuscript to a SpringerOpen journal and benefit from:

- ► Convenient online submission
- ► Rigorous peer review
- ► Open access: articles freely available online
- ► High visibility within the field
- ► Retaining the copyright to your article

Submit your next manuscript at ► springeropen.com